ELSEVIER

Polymer 41 (2000) 5985–5992

polymer

Miscibility and solid-state structures for blends of poly[(*S*)-lactide] with atactic poly[(*R*,*S*)-3-hydroxybutyrate]

I. Ohkoshi[a], H. Abe[b], Y. Doi[b,*]

[a]*Material Research Center, Riken Vinyl Industry Co. Ltd, Minami-Rokugou, Ohta-ku, Tokyo 144-0045, Japan*
[b]*Polymer Chemistry Laboratory, The Institute of Physical and Chemical Research (RIKEN), 2-1 Hirosawa, Wako-shi, Saitama 351-0198, Japan*

Received 20 August 1999; received in revised form 7 October 1999; accepted 17 October 1999

Abstract

The miscibility and phase structure of binary blends of poly[(*S*)-lactide] (PLA) ($M_w = 680,000$) with atactic poly[(*R*,*S*)-3-hydroxybutyrate] (ataPHB) of different molecular weights ($M_w = 9400$, 21,000 and 140,000) have been investigated by the means of differential scanning calorimetry (DSC) and optical microscopy. DSC thermograms for the blends of PLA and ataPHB with $M_w = 9400$ in the range from 0 to 50 wt.% of ataPHB content showed single glass transition temperature after melting at 200°C, and the value decreased from 59 to 10°C with an increase in the ataPHB content, indicating that the PLA and low molecular weight ataPHB ($M_w = 9400$) are miscible in the melt at 200°C within the ataPHB content up to 50 wt.%. In contrast, the binary blends of PLA with high molecular weight ataPHB ($M_w = 140,000$) showed two glass transition temperatures indicating that the binary blend is immiscible in the melt. The radial growth rate of PLA spherulites were accelerated by the addition of low molecular weight ataPHB components. The solid-state structures of melt-crystallized films for miscible blend of PLA with low molecular weight ataPHB were characterized by DSC, wide-angle X-ray diffraction, small-angle X-ray scattering and dynamic mechanical thermal analysis. X-ray crystallinities of PLA components in the melt-crystallized films were increased by the addition of small amount of ataPHB component, suggesting that the addition of small amount of ataPHB-3 component facilitated the crystallization of PLA components in the binary blends. The lamellar thickness of PLA crystals decreased slightly with an increase in ataPHB content, suggesting that ataPHB component was incorporated into the interlamellar region of PLA spherulites. The relaxation phenomena were detected at two different temperatures in the dynamic mechanical spectra for PLA/ataPHB blends (containing ataPHB contents over 15 wt.%) crystallized at 120°C, indicating that the partial phase separation of two components occurs in the amorphous phase during the isothermal crystallization process.

Keywords: Poly[(*S*)-lactide]; Atactic poly[(*R*,*S*)-3-hydroxybutyrate]; Polymer blend

1. Introduction

Poly[(*S*)-lactide] (PLA) is synthesized from either lactic acid or its cyclic dimer [1–6] and is a biodegradable and biocompatible thermoplastic with a melting point around 180°C. PLA has been investigated as a material for medical devices such as controlled drug release matrices [7,8], degradable sutures [9,10] and implanted for bone fixation [11]. The degradation of PLA in an aqueous environment is mainly due to non-enzymatic hydrolysis of polymer chains catalyzed by carboxyl end groups of polymers to generate monomer and oligomers of lactic acid, which can be metabolized by many microorganisms [12]. Therefore, there is increasing interest in using PLA as an environmentally degradable plastic material.

Several approaches such as copolymerization [13], blending and processing [14] have been extensively studied to produce PLA-based materials with a wide range of physical properties and improved processability. Blends of PLA with poly(ϵ-caprolactone) [15,16], poly[(*R*)-3-hydroxybutyrate] [17,18], poly[(*R*)-3-hydroxybutyrate-*co*-(*R*)-3-hydroxyvalerate] [19], poly(ethylene oxide) [20–22], poly(vinyl acetate) [23], and poly(*p*-vinyl phenol) [24] have been investigated. Many fundamental studies have dealt with the miscibility of blends in the melt. Since PLA is a semicrystalline polymer, the crystallized blends with amorphous polymers are composed of crystalline and amorphous phases. The solid-state structures of blends may be strongly dependent on the miscibilities at both the mixing and the crystallization temperatures. However, the solid-state structures for blends of semicrystalline PLA and amorphous polymers have been reported in few studies.

Atactic poly[(*R*,*S*)-3-hydroxybutyrate] (ataPHB) is

* Corresponding author. Tel.: +81-48-467-9402; fax: +81-48-462-4667.
E-mail address: ydoi@postman.riken.go.jp (Y. Doi).

0032-3861/00/$ - see front matter
PII: S0032-3861(99)00781-8

synthesized by the polymerization of racemic β-butyrolactone and is a completely amorphous polymer. It has been found that ataPHB polymer chains blending with semicrystalline polymers such as poly[(*R*)-3-hydroxybutyrate], poly(ϵ-caprolactone) and PLA are hydrolyzed by the function of PHB degrading enzyme, while the enzyme hardly hydrolyzes the pure ataPHB, suggesting that the presence of stable crystalline phase induces the enzymatic hydrolysis of amorphous ataPHB chains [25,26].

In this paper, we investigate the miscibility for binary blends of PLA with ataPHB of various molecular weights ($M_w = 9400$–$140,000$) in the melt at 200°C. The solid-state structures of melt-crystallized films for the blends of PLA with ataPHB are characterized, and the crystallization behavior of PLA component and the phase separation phenomenon in amorphous region during the isothermal crystallization process are discussed.

2. Experimental

2.1. Materials

Poly[(*S*)-lactide] (PLA; $M_w = 778,000$, $M_w/M_n = 2.3$ by gel permeation chromatography) was purchased from Polyscience and used as received without further purification. Poly[(*R,S*)-3-hydroxybutyrate] (ataPHB-1; $M_w = 140,000$, $M_w/M_n = 1.5$, ataPHB-2; $M_w = 21,000$, $M_w/M_n = 1.2$, and ataPHB-3; $M_w = 9400$, $M_w/M_n = 1.6$), synthesized as described previously [25], was found to be atactic by ^{13}C nuclear magnetic resonance spectroscopy.

2.2. Blend preparation

Solvent-cast films of binary blends of PLA with ataPHB were prepared by dissolving the polymeric binary mixtures in chloroform and casting on glass plates at room temperature for 1 week, and then dried under reduced pressure. The films were inserted between two Teflon sheets (0.2 mm thickness) with a Teflon sheet (0.2 mm thickness) as a spacer and compression-molded on a Mini Test Press (Toyoseiki) by heating at 200°C for 1 min under a pressure of 75 kg cm^{-2}. After melting, samples were kept at a given crystallization temperature (T_c) and isothermally crystallized for 3 days. The melt-crystallized films were about 0.2 mm in thickness and stored at −20°C until needed.

2.3. Analytical procedures

All molecular weight data were obtained by gel permeation chromatography at 40°C, using a Shimadzu 10A system and a 6A refractive index detector with Shodex K-802 and K-806M columns. Chloroform was used as an eluent at a flow rate of 0.8 ml min^{-1}, and a sample concentration of 1.5 mg ml^{-1} was applied. Polystyrene standards with low polydispersity were used to prepare the calibration curve.

The DSC data were recorded in the temperature range of −100–200°C under a nitrogen flow rate of 30 ml min^{-1} on a Shimadzu DSC-50Q instrument equipped with a cooling accessory. The solvent-cast films (5 mg) were encapsulated in aluminum pans and heated from 0 to 200°C at a heating rate of 10°C min^{-1} (1st scan). Then the melt samples were maintained at 200°C for 1 min and followed by rapid quenching at −100°C. They were then heated from −100 to 200°C at a heating rate of 20°C min^{-1} (2nd scan). The glass transition temperature (T_g) was taken as the midpoint of the heat capacity change. The cold crystallization peak temperature (T_{cc}) was determined from the DSC exotherm, whereas the melting temperature (T_m) and the enthalpy of fusion (ΔH_m) were determined from the DSC endotherm. For the melt-crystallized films, DSC scans were carried out from −100 to 200°C at a heating rate of 20°C min^{-1} to determine the T_m and ΔH_m.

The morphologies of PLA spherulites were observed with an optical microscope (Nikon OPTIPHOTO-2) equipped with crossed polarizers, a Linkam hot stage, a CCD camera (Ikegami IF-8500) and an image analyzer (OLYMPUS XL-10). The solvent-cast films were first heated on a hot stage from room temperature to 200°C at a rate of 30°C min^{-1}. The samples were maintained at 200°C for 1 min, and then the temperature was rapidly lowered to a given temperature (T_c). The samples were crystallized at a given T_c to monitor the growth of spherulites as a function of time. The radial growth rate of PLA spherulites (G) was calculated as the slope of the line obtained by plotting the spherulite radius against time with more than ten data points.

The wide angle X-ray diffraction (WAXD) patterns of melt-crystallized films were recorded at 25°C on a Rigaku RINT 2500 system using nickel-filtered Cu Kα radiation ($\lambda = 0.154$ nm; 40 kV; 200 mA) in the 2θ range of 6–40° at a scanning speed of 2.0° min^{-1}. Degree of crystallinity (X_c) of the blend films was calculated from the diffracted intensity data according to Vonk's method [27].

The small angle X-ray scattering (SAXS) patterns of melt-crystallized films were recorded at 25°C on a Rigaku RINT 2500 system using Cu Kα radiation ($\lambda = 0.154$ nm; 40 kV; 200 mA) in the 2θ range of 0.1–3.0° at a scanning speed of 0.05° min^{-1}. Since the SAXS data are collected in a limited angular range, it must necessarily be extrapolated to both high and low angular ranges before Fourier transformation [28,29]. The extrapolation to high angular range was performed using Porod's law. For low angular extrapolation, the straight-line relationship between 0 and lower limit of SAXS measurement was assumed.

Dynamic mechanical spectra of melt-crystallized films were recorded at a heating rate of 2°C min^{-1} and a frequency of 1 Hz in the temperature range of −100–200°C, using a Seiko Instruments DMS210 dynamic mechanical thermal analyzer.

Table 1
Thermal properties of PLA/ataPHB blends

Sample	Composition (w/w)	T_g[a] (°C)	T_{cc}[b] (°C)
PLA/ataPHB-1	100/0	59	138
$M_w = 140,000$	95/5	5,58	131
$M_w/M_n = 1.5$	85/15	0,56	123
	75/25	1,56	115
	50/50	1,54	113
	0/100	0	
PLA/ataPHB-2	100/0	59	138
$M_w = 21,000$	95/5	55	112
$M_w/M_n = 1.2$	85/15	48	100
	75/25	3,49	99
	50/50	2,46	104
	0/100	−8	
PLA/ataPHB-1	100/0	59	138
$M_w = 9400$	95/5	53	119
$M_w/M_n = 1.6$	85/15	41	91
	75/25	29	84
	50/50	10	77
	40/60	−2,10	74
	0/100	−16	

[a] Glass transition temperature measured by DSC (2nd run) from −100 to 200°C at a rate of 20°C min^{-1}.
[b] Cold crystallization peak temperature measured by DSC (2nd run).

3. Results and discussion

3.1. Miscibility of PLA/ataPHB blends in the melt at 200°C

The glass transition temperatures (T_g) of binary blends of PLA with ataPHB were determined by DSC measurements, and the data are summarized in Table 1. Fig. 1 shows the DSC thermograms (2nd scan) for blends of PLA with ataPHB of different molecular weights. The T_g values of PLA with high molecular weight ataPHB (ataPHB-1; $M_w = 140,000$) were, respectively, 59 and 0°C, and the T_g values of both components in the PLA/ataPHB-1 blends were almost independent of the blend composition, indicating that the binary blend is immiscible in the melt at 200°C.

DSC thermograms for PLA with low molecular weight ataPHB (ataPHB-3; $M_w = 9400$) showed single glass transition temperature within the ataPHB content up to 50 wt.%, and the value decreased from 59 to 10°C with an increase in the ataPHB content. The relationship between T_g value of PLA/ataPHB-3 blends and the blend composition is illustrated in Fig. 2. For miscible polymer blends their T_g value can be expressed by Wood's equation [30] (Eq. (1))

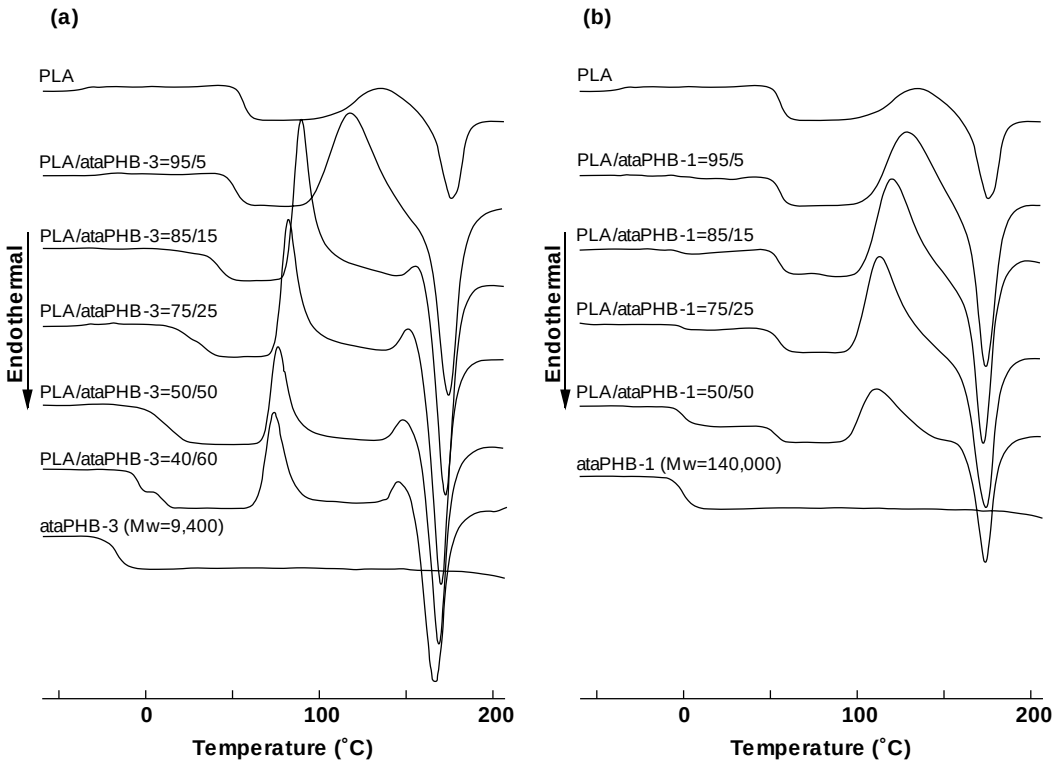

Fig. 1. DSC thermograms (2nd run) of PLA/ataPHB blends at a rate of 20°C min^{-1}: (a) blend of PLA with low molecular weight ataPHB-3 ($M_w = 9400$); and (b) blend of PLA with high molecular weight ataPHB-1 ($M_w = 140,000$).

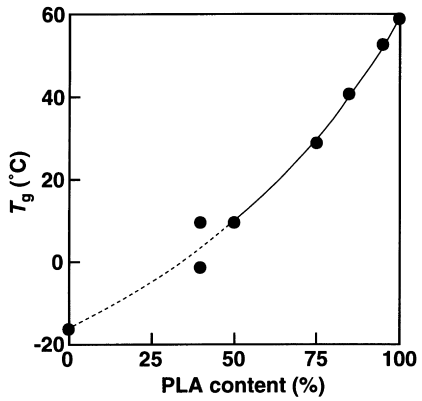

Fig. 2. Glass transition temperature (T_g) of the blend of PLA with low molecular weight ataPHB-3.

with the k parameter treated as an empirical adjustable parameter

$$T_g = (w_1 T_{g1} + k w_2 T_{g2})/(w_1 + k w_2) \quad (1)$$

where w_1 and w_2 are, respectively, the weight fractions of PLA and ataPHB-3, and T_{g1} and T_{g2} are, respectively, the glass transition temperatures of PLA and ataPHB-3. The experimental T_g values of ataPHB-3 content ranging from 0 to 50 wt.% are in good agreement with the curve calculated by Wood's equation with k value of 1.9. This result indicates that PLA is miscible with low molecular weight ataPHB-3 in the melt at 200°C within the ataPHB content up to 50 wt.%. However, the PLA with 60 wt.% of ataPHB-3 showed the two different T_gs at 10 and −2°C, suggesting a biphasic separation in the melt.

The blends of PLA and ataPHB-2 ($M_w = 21,000$) showed the two different T_gs corresponding to the molecular relaxations from PLA and ataPHB-2 components, suggesting a biphasic separation in the melt at 200°C. However, the T_g value arising from PLA component dropped with an addition of ataPHB-2 component up to 15 wt.%, suggesting the partial dispersion of ataPHB-2 component in PLA phase. From these results, we have concluded that the miscibility for binary blends of PLA with ataPHB is strongly dependent on the molecular weight of ataPHB component.

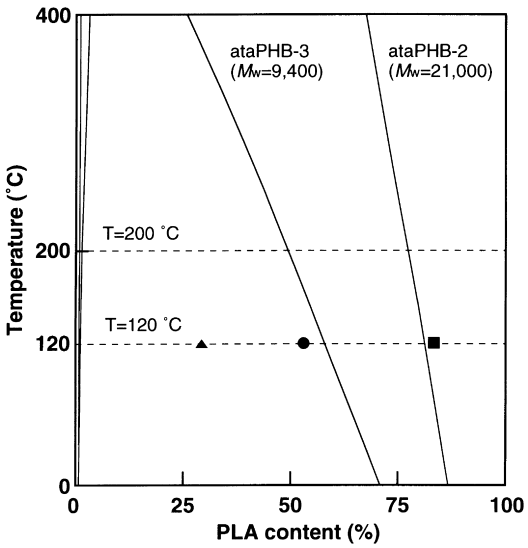

Fig. 3. Spinodal curves for the binary blends of PLA with ataPHB calculated using the Flory–Huggins equation with the difference in solubility parameters of 0.58 $(J\,cm^{-3})^{1/2}$. The PLA content in amorphous phase of melt-crystallized films crystallized at 120°C: PLA/ataPHB-3 = 95/5 (w/w) (■); 85/15 (w/w) (●); and 75/25 (w/w) (▲).

The cold crystallization peak temperature (T_{cc}) of PLA components was determined from DSC curves (2nd scan). The results are given in Table 1. The T_{cc} values of PLA component in the blends with ataPHB of Mw values of 21,000 and 140,000 decreased slightly with an increase in ataPHB content. In contrast, the T_{cc} values of PLA component in the PLA/ataPHB-3 blends decreased remarkably from 138 to 77°C as the ataPHB-3 content was increased from 0 to 50 wt.%. The depression of the T_{cc} values for the blends of PLA with low molecular weight ataPHB-3 can be explained, considering that the crystallization process takes place from the single homogeneous phase.

As described above, the miscibility of PLA with ataPHB is strongly dependent on both the molecular weight of ataPHB component and blend composition. The effect of the molecular weight of ataPHB component on the miscibility of PLA/ataPHB blends can be understood on the basis of Flory–Huggins equation [31] (Eq. (2))

$$\frac{\Delta G}{RTV} = \frac{\phi_1}{N_1}\ln \phi_1 + \frac{\phi_2}{N_2}\ln \phi_2 + \chi_{12}\phi_1\phi_2 \quad (2)$$

where ΔG is the change of free energy by mixing of two polymers, R the gas constant, V the volume of mixing system, ϕ_1 and ϕ_2 are, respectively, the volume fractions of PLA and ataPHB, N_1 and N_2 are, respectively, the molar volumes of PLA and ataPHB, and χ_{12} is the Flory interaction parameter. By assuming no specific interaction between PLA and ataPHB molecules, the interaction parameter χ_{12} is expressed by the equation using the solubility parameters(δ_1 and δ_2 of blend components (Eq. (3)).

$$\chi_{12} = \frac{(\delta_1 - \delta_2)^2}{RT} > 0 \quad (3)$$

The difference of the solubility parameters, $(\delta_1 - \delta_2)$, can be estimated from the spinodal ($\partial^2 \Delta G/\partial \phi^2 = 0$) on the basis of the relationship between the miscibility and the molecular weight of ataPHB component. PLA is miscible with low molecular weight ataPHB-3 in the melt at 200°C within the ataPHB content up to 50 wt.%, while the PLA with 60 wt.% of ataPHB-3 showed a biphasic separation. Thus, the difference in the solubility parameters of blend components in the Flory–Huggins equation was estimated to be 0.58 $(J\,cm^{-3})^{1/2}$, and the spinodal curves for the binary blends of PLA with ataPHB were established (Fig. 3). As shown in Fig. 3, PLA is miscible with ataPHB-3 in the range of 0–50 wt.% at the temperature (200°C) of the melting blends.

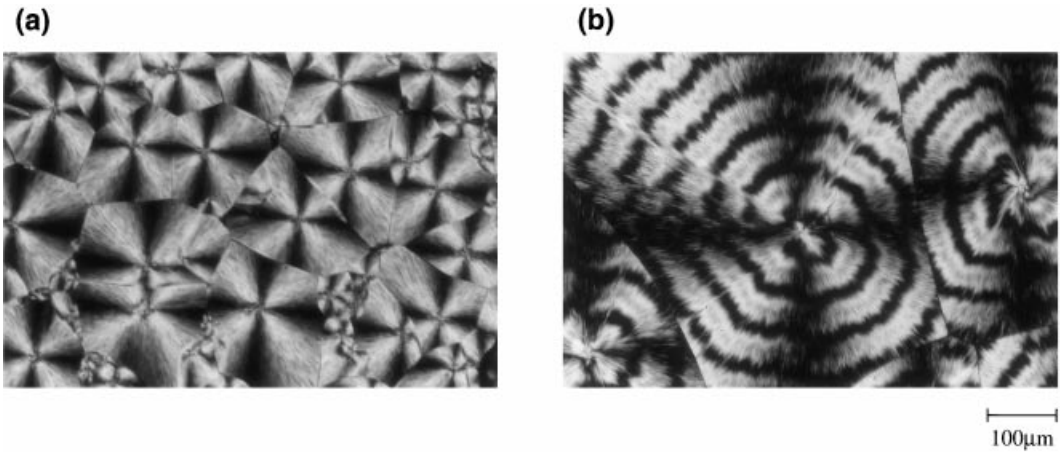

Fig. 4. Optical micrographs of PLA spherulites for: (a) pure PLA; and (b) PLA/ataPHB-3 = 75/25 (w/w) blend crystallized at 130°C.

3.2. Spherulitic morphologies for PLA/ataPHB blends

Spherulitic morphologies for the binary blends of PLA with ataPHB were characterized by a cross-polarized optical microscopy. Samples were isothermally crystallized at a given crystallization temperature after melting at 200°C. There was no evident slowing of the growth fronts as the spherulites impinge. The spherulite radius increased linearly with time. The radial growth rate depended on both the crystallization temperature and the blend composition. Fig. 4 shows the typical optical micrographs of the PLA spherulites for pure PLA and PLA/ataPHB-3 = 75/25 (w/w) crystallized at 130°C. After crystallization at 130°C from the melt at 200°C, PLA/ataPHB blends showed the spherulitic morphology of PLA components. For the miscible blends of PLA/ataPHB-3, there was no evidence of biphasic separation, and the impinging PLA spherulites were observed. This result indicates that the ataPHB-3 component is trapped into PLA spherulites. PLA spherulites in the PLA/ataPHB-3 = 75/25 (w/w) blend showed the obvious banding morphology. However, the banding texture was not apparent in the spherulites of pure PLA. It is suggested that the addition of ataPHB-3 induces the periodic torsion of growing PLA lamellae. Same behavior has already been reported by Scandola et al. [26].

Fig. 5 shows the radial growth rate of PLA spherulites (G) for pure PLA and PLA/ataPHB blends at different crystallization temperatures (T_c). A maximum value (4.2 μm min^{-1}) of G was observed near 130°C for pure PLA. The radial growth rate of PLA spherulites (G) for immiscible blends of PLA with ataPHB-1 was dependent on the crystallization temperature, while the rate was independent of the blend composition. In contrast, the growth rate was accelerated by the addition of ataPHB component for the miscible blends of PLA with ataPHB-3, and a maximum G value of 12.2 μm min^{-1} was observed near 110°C.

In most cases of miscible blends of crystallizable/non-crystallizable polymers, the crystal growth rate of crystallizable component is depressed by the mixing of amorphous component. The depression of crystal growth is attributed to the diluent effect of the non-crystallizable component. However, in this study the growth rate of PLA spherulites was accelerated by the addition of the non-crystallizable ataPHB-3 component. The chain mobility of crystallizable

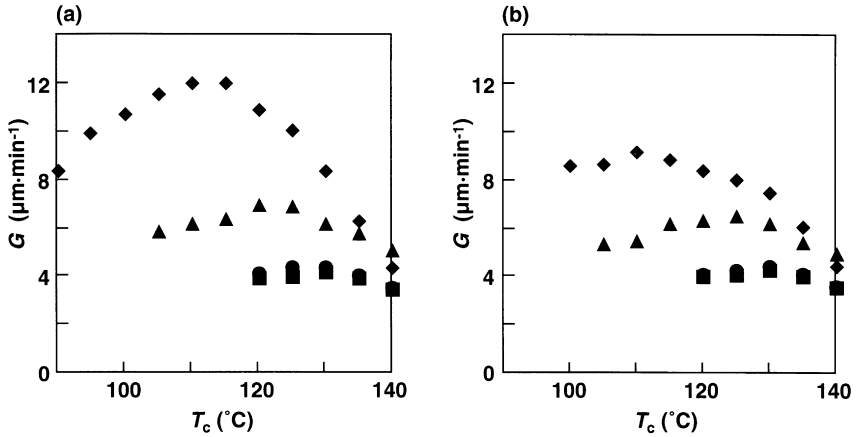

Fig. 5. Radial growth rate of PLA spherulites (G) as a function of crystallization temperature (T_c) for: (a) PLA and PLA/ataPHB = 50/50 (w/w) blends and (b) PLA and PLA/ataPHB = 75/25 (w/w) blends: (■) PLA; (●) PLA/ataPHB-1; (▲) PLA/ataPHB-2; and (◆) PLA/ataPHB-3.

Table 2
Thermal properties of PLA/ataPHB melt crystallized blend films

Sample	Composition (w/w)	$T_c = 90°C$[a]			$T_c = 120°C$			$T_c = 140°C$		
		T_m[b] (°C)	ΔH_m[c] (J·g^{-1})	X_c[d] (%)	T_m (°C)	ΔH_m (J g^{-1})	X_c (%)	T_m (°C)	ΔH_m (J g^{-1})	X_c (%)
PLA/ataPHB-3	100/0	178	32	42	179	51	52	184	58	64
$M_w = 9400$	95/5	179	38	47	179	64	69	183	75	78
$M_w/M_n = 1.6$	85/15	178	41	43	177	56	68	179	74	77
	75/25	175	37	39	174	55	65	177	67	69

[a] Crystallization temperature.
[b] Melting temperature measured by DSC (1st run) from 0 to 200°C at a rate of 20°C min^{-1}.
[c] Enthalpy of fusion measured by DSC (1st run).
[d] X-ray crystallinity measured by WAXD.

component also affects the rate of crystal growth owing to the changes in activation energy to transport the crystallizable polymer segments towards the growing front of lamellar crystals. The viscosity of low molecular weight ataPHB-3 ($M_w = 9400$) was much lower than that of PLA ($M_w = 680,000$) in the crystallization process. Therefore, the chain mobility of crystallizable PLA component may be increased by the addition of ataPHB-3 component. In the case of miscible PLA/ataPHB-3 blend, the acceleration of the growth rate of PLA spherulites may be attributed to the increase in chain mobility of the crystallizable PLA component by the addition of ataPHB-3 component.

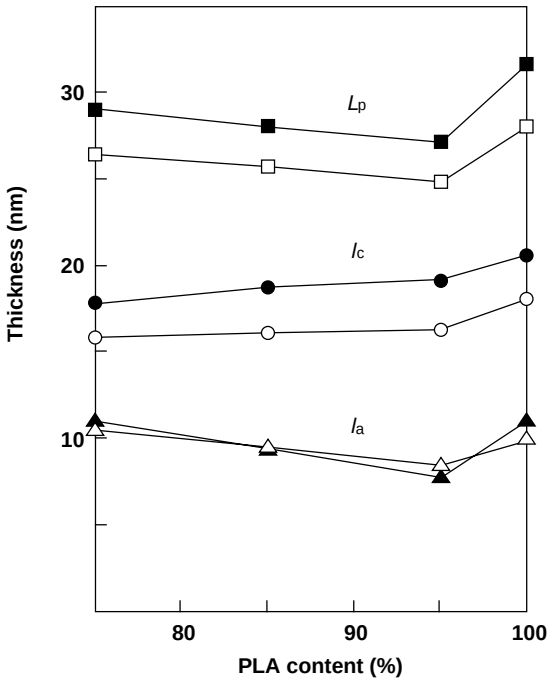

Fig. 6. Plots of long period (L_p), lamellar thickness (l_c), and amorphous thickness (l_a) of the melt-crystallized PLA/ataPHB-3 blends as a function of PLA content. Symbols: (square) long period, (circle) lamellar thickness, (triangle) amorphous thickness; (closed) crystallized at 140°C, (open) crystallized at 120°C.

3.3. Solid-state structures of PLA/ataPHB blends

Melt-crystallized films for miscible blends of PLA with ataPHB-3 were prepared by isothermally crystallizing at 90, 120 and 140°C from the melt at 200°C. After crystallization for 3 days, all binary blend films showed the well-developed and volume-filled PLA spherulites.

Thermal properties of melt-crystallized films for miscible blends of PLA with ataPHB-3 were characterized by DSC measurements, and the data are listed in Table 2. The T_m values of PLA crystalline increased with a rise in the crystallization temperature from 90 to 140°C. The T_m values of PLA crystalline in PLA/ataPHB-3 blends crystallized at an identical crystallization temperature depressed with an increase in ataPHB-3 composition, suggesting that the thickness of PLA lamellar crystals decreased by the addition of ataPHB-3 composition.

The ΔH_m values of the melt-crystallized films for miscible PLA/ataPHB-3 blends increased with a rise in crystallization temperature. ΔH_m values of the melt-crystallized films crystallized at an identical crystallization temperature increased by the addition of small amount of ataPHB-3 component, and the maximum values were observed at ataPHB-3 content of 5 wt.%.

The crystalline structure of melt-crystallized films for miscible PLA/ataPHB-3 blends was characterized by WAXD analysis. The diffraction patterns of all samples showed reflections arising from the crystalline lattice of PLA crystal. X-ray crystallinities (X_c) of PLA components in the melt-crystallized films were calculated from the diffraction patterns, and the data are listed in Table 2. The X_c values of binary blends increased with an increase in ataPHB-3 content up to 5 wt.% to reach a maximum value followed by a decrease in the crystallinity. The X_c values showed a similar trend to the ΔH_m values of melt-crystallized blend films.

The radial growth rate of PLA spherulites for miscible PLA/ataPHB-3 blend increased by the addition of ataPHB-3 component up to 50 wt.%. In addition, the crystallinity of PLA component in the melt-crystallized films crystallized at an identical crystallization temperature increased with an increase in ataPHB-3 content. For example, the crystallinity

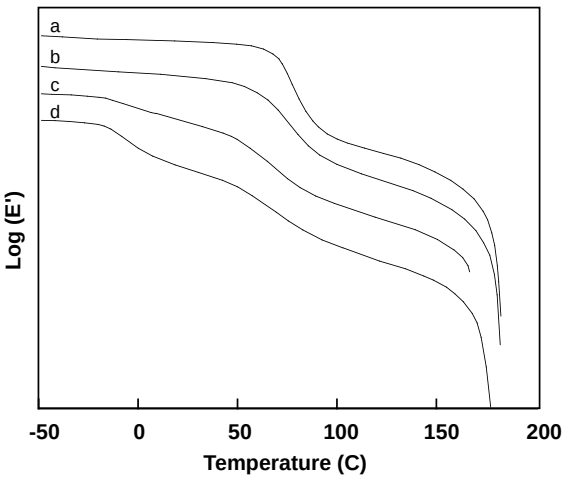

Fig. 7. Dynamic mechanical spectra of PLA/ataPHB-3 blend crystallized at 120°C: (a) pure PLA; (b) PLA/ataPHB-3 = 95/5 (w/w); (c) PLA/ataPHB-3 = 85/15 (w/w); (d) PLA/ataPHB-3 = 75/25 (w/w).

of PLA component in melt-crystallized films crystallized at 120°C increased from 52 to 87% as the ataPHB content was increased from 0 to 25 wt.%. These results suggest that the addition of ataPHB-3 component facilitated the crystallization of PLA components in the binary blends.

The lamellar structure of melt-crystallized films for miscible PLA/ataPHB-3 blends was characterized by SAXS analysis. In general, we can obtain the lamellar thickness value from the long period and crystallinity. However, the crystallinity determined from WAXD may be the overall value including both lamellar crystals and crystallites. Therefore, in this study, to estimate the long period distance (L_p), lamellar thickness (l_c) and amorphous layer thickness (l_a) of the PLA lamellar stacks in the melt-crystallized blend films, the scattering data were analyzed according to the pseudo two-phase model using one-dimensional correlation function, which can be taken directly as the Fourier transform of the scattering intensity (see Section 2). Fig. 6 shows the relationships between the blend composition and the L_p, l_c and l_a values. The L_p value of PLA crystals decreased by the addition of 5 wt.% of ataPHB-3 component, and then the L_p value increased as the ataPHB-3 composition was increased from 5 to 25 wt.%. The l_c values of PLA crystals decreased slightly with an increase in the ataPHB-3 content, and this result was in good agreement with the depression of T_m values of PLA crystalline in PLA/ataPHB-3 blends. The l_a value decreased by the addition of 5 wt.% of ataPHB-3 component, and then the l_a value increased as the ataPHB-3 composition was increased from 5 to 25 wt.%. In contrast, the X-ray crystallinity values showed an opposite trend to the L_p and l_a values of melt-crystallized blend films. As a result, the non-crystallizable ataPHB-3 component was trapped not only into interfibrillar regions, but also into interlamellar regions of the PLA spherulites.

Dynamic mechanical thermal measurements were carried out on the melt-crystallized films for PLA/ataPHB-3 blends crystallized at 120°C. Fig. 7 shows the dynamic storage modulus of the melt-crystallized films for PLA/ataPHB-3 blends crystallized at 120°C. The relaxation phenomenon associated with the glass transition of amorphous phase was observed in the dynamic mechanical spectra, evidenced by the drop of the modulus. The drop of storage modulus was observed around 75°C corresponding to the glass transition of the PLA amorphous region for pure PLA. For PLA/ataPHB-3 = 95/5 (w/w) blend, single modulus drop was shown at around 68°C in the dynamic mechanical spectra, indicating that the PLA component was miscible with the ataPHB-3 component in the amorphous phase during the isothermal crystallization process at 120°C. On the contrary, the relaxation phenomena were detected at two different temperature ranges at −5 and 60°C for PLA/ataPHB-3 = 85/15 and 75/25 (w/w) blends, indicating that the partial phase separation of two components occurs in the amorphous phase.

As shown in Fig. 3, the PLA/ataPHB-3 blends of ataPHB-3 content ranging from 0 to 25 wt.% form a single homogeneous phase at 0°C and over. However, the amorphous phase in the melt-crystallized films for PLA/ataPHB-3 = 85/15 and 75/25 (w/w) exhibited the phase separations, as a result of dynamic mechanical thermal analysis. The PLA components in the binary blends were crystallized at 120°C, and the non-crystallizable ataPHB-3 components were concentrated in the amorphous phase. The PLA content in the amorphous region of the melt-crystallized blend films was calculated from the crystallinity of blend films. The PLA contents in the amorphous region of melt-crystallized PLA/ataPHB-3 = 95/5, 85/15 and 75/25 (w/w) blends crystallized at 120°C were 84, 53 and 29 wt.%, respectively. The PLA contents in the amorphous region for PLA/ataPHB-3 = 85/15 and 75/25 (w/w) blend films were less than the PLA content (58 wt.%) limited to form the homogeneous phase at 120°C. Consequently, the partial phase separation of two components may occur in the amorphous phase during the isothermal crystallization process at 120°C for PLA/ataPHB-3 = 85/15 and 75/25 (w/w) blends. It is concluded that the melt-crystallized films for PLA/ataPHB-3 = 95/5 (w/w) blend crystallized at 120°C formed the two phases of PLA crystalline phase and homogeneous amorphous phase of 84 wt.% PLA content, while the PLA/ataPHB-3 = 85/15 and 75/25 (w/w) blends formed the three phases of PLA crystalline phase, amorphous phase with relatively higher PLA content and ataPHB-3 phase.

References

[1] Kleine J, Kleine H-H. Makromol Chem 1959;30:23.
[2] Vert M, Christel P, Chabot F, Leray J. In: Hasting GW, Ducherne P, editors. Macromolecular biomaterials, Boca Raton, FL: CRC Press, 1984. pp. 119–42.
[3] Jamshidi K, Eberhart RC, Hyon S-H, Ikada Y. Polym Prepr 1987;28:236.
[4] Leenslag JW, Pennings AJ. Makromol Chem 1987;188:1909.

[5] Sipos L, Zsuga M, Kelen T. Polym Bull 1992;27:295.
[6] Ajioka M, Enomoto K, Suzuki K, Yamaguti A. Bull Chem Soc Jpn 1995;68:2125.
[7] Jackanicz TM, Nash HA, Wise DL, Gregory JB. Contraception 1973;8:227.
[8] Arshady R. J Control Release 1991;17:1.
[9] Penning JP, Dijkstra H, Pennings AJ. Polymer 1993;34:942.
[10] Vainionpaa S, Rokkamen P, Tormala P. Prog Polym Sci 1989;14:679.
[11] Ikada Y, Shikinami Y, Hara Y, Tagawa M, Fukuda E. . J Biomed Mater Res 1996;30:553.
[12] Shih C. J Control Release 1995;34:9.
[13] Jedlinski Z, Kurcok P, Lenz RW. J Macromol Sci Pure Appl Chem 1995;A32:797.
[14] Datta R, Tsai S-P, Bonsignore P, Moon S-H, Frank JR. FEMS Microbiol Rev 1995;16:221.
[15] Hiljanen-Vainio M, Varpomaa P, Seppala J, Tormala P. Macromol Chem Phys 1996;197:1503.
[16] Tsuji H, Ikada Y. J Appl Polym Sci 1996;60:2367.
[17] Koyama Y, Doi Y. Polymer 1997;38:1589.
[18] Zhang LL, Xiong CD, Deng XM. Polymer 1996;37:235.
[19] Iannace S, Ambrosio L, Huang SJ, Nicolais L. J Appl Polym Sci 1994;54:1525.
[20] Nakafuku C, Sakoda M. Polym J 1993;25:909.
[21] Nakafuku C. Polym J 1996;28:568.
[22] Nijenhuis AJ, Colstee E, Grijpma DW, Pennings AJ. Polymer 1996;37:5849.
[23] Gajria AM, Dave V, Gross RA, McCarthy SP. Polymer 1996;37:437.
[24] Zhang L, Goh SH, Lee SY. Polymer 1998;39:4841.
[25] Abe H, Matsubara I, Doi Y. Macromolecules 1995;28:844.
[26] Focarete ML, Ceccorulli G, Scandola M, Kowalczuk M. Macromolecules 1998;31:8485.
[27] Vonk CG. J Appl Crystallogr 1973;6:148.
[28] Vonk CG. J Appl Crystallogr 1975;8:340.
[29] Verma R, Marand H, Hsiao B. Macromolecules 1996;29:7767.
[30] Wood LA. J Polym Sci 1958;28:319.
[31] Flory PJ. Principles of polymer chemistry, Ithaca, NY: Cornell University Press, 1953.